Hindawi
Mathematical Problems in Engineering
Volume 2020, Article ID 1392380, 8 pages
https://doi.org/10.1155/2020/1392380

Research Article

Friction Torque Analysis of Planetary Roller Screw Mechanism in Roller Jamming

Linjie Li[1], **Yongling Fu**[1], **Shicheng Zheng**[1], **Jian Fu**[1] and **Tianxiang Xia**[2]

[1]*School of Mechanical Engineering and Automation, Beihang University, Beijing 100083, China*
[2]*Nanjing Engineering Institute of Aircraft System Jincheng, AVIC, Nanjing 211100, China*

Correspondence should be addressed to Jian Fu; fujian@buaa.edu.cn

Received 21 September 2019; Revised 14 January 2020; Accepted 24 January 2020; Published 20 March 2020

Academic Editor: Vasilios Spitas

The load distribution model of the planetary roller screw mechanism (PRSM) is established on the basis of Hertz contact theory. The objective is to obtain a friction torque model of the PRSM in roller jamming. An example is provided to calculate the friction torque of the PRSM in roller jamming. Thereafter, the transmission efficiency is calculated. A static structural analysis is performed using the finite element method to estimate the contact stress between the threads of the PRSM components. Computational results indirectly reveal that roller jamming exerts considerable influence on the friction torque of the PRSM. Results show that the friction torque of the planetary roller screw increases when the roller is jammed and the wear of the parts is accelerated. This condition leads to structural failure. The results of this study can serve as a foundation for electromechanical actuation systems, which can be useful in designing antijamming systems for safety-critical aircraft applications.

1. Introduction

Electromechanical actuators (EMAs) are widely used in the field of aerospace actuation for flight control, landing gear, trimmable horizontal stabilizer, and thrust reverser [1–3]. The mechanical parts of an EMA mainly include an electrical motor, gear, and components for transforming the rotational motion of the motor into a linear one to actuate the control surface [4, 5]. Planetary roller screws are commonly used to transform the rotational motion into a linear one (Figure 1).

The planetary roller mechanism transforms the rotary motion into a linear one through the threaded surface contacts of the components. During its operation, the force and motion are transferred through the threaded surfaces. The PRSM has many advantages over the ball screw mechanism, and these advantages include high precision, low sensitivity to impact load, and high reliability in severe environments.

Friction torque, an important technical index to evaluate the performance of the PRSM, has received increasing attention in the application field of such mechanisms. The friction torque of the PRSM has been studied by many scholars. For example, friction torque is not only related to mechanism size but also influenced by the load and viscosity of the lubrication in the roller drive mechanism [7]. Hojjat and Mahdi Agheli pointed out that the friction of the roller screw mechanism is a combination of sliding and rolling friction. However, this study did not analyze the effects of sliding friction on external loads [8]. Velinsky et al. explained that the contact radii between the roller thread and the lead screw and nut threads are not identical and deduced the contact radius of the lead screw, the roller, and the nut [9]. Matthew presented an efficiency model of the roller screw mechanism [10]; the relationship between the direction of friction force and the sideslip speed was studied, and the viscous friction model of the roller screw mechanism was derived [11]. However, the influence of load on friction torque was ignored; thus, the model is only suitable for unloaded conditions. Zhang et al. [12] studied the influence of different installation methods, stress state, structural parameters, and other factors on the load distribution of PRSM. Yang et al. [13] studied the effects of the preloading of the roller screw mechanism on its axial deformation and

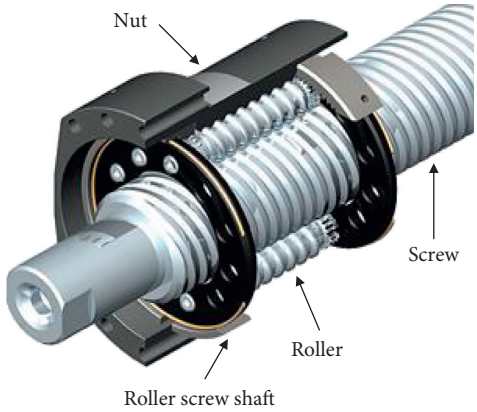

Figure 1: Planetary roller screw mechanism (PRSM) [6].

friction, but only the elastic lag and friction moment of the rolling spin part were considered in the mathematical model of friction moment; all other factors were neglected. Li et al. also studied the influence of the thread contact angle and spiral rising angle on the transfer efficiency of the roller screw mechanism [14]. Ma et al. studied the qualitative relationship between external load and speed and friction torque [15] and transmission efficiency of the roller screw mechanism [16] and established a friction torque model [17]. However, the effects of load on the friction coefficient are neglected in the aforementioned model. Pu and Fan [18] studied in detail the friction of the roller screw mechanism but did not explore the influence of structural parameters on friction moment. The friction of the roller screw is a combination of rolling and sliding. However, the friction moment of roller failure, such as roller jamming, is seldom reported in the literature. The friction torque of the PRSM in the roller failure mode is studied in the current work on the basis of the analysis of the friction torque modeling of the PRSM.

2. Friction Moment Model

The friction moment of the PRSM is mainly caused by elastic hysteresis resistance, differential sliding between the roller and the raceway, spin sliding, and viscous resistance of lubrication [17]. Herein, the engagement between the roller and the lead screw and nut is studied. The force between the roller and the ring gear and cage is actually small, and the friction torque produced in this part is ignored.

2.1. Load Distribution of PRSM. Figure 2 shows a force analysis of PRSM in contact with a single mechanism of threads under the loads of axial force F_{ai}, radial force F_{ri}, and tangential force F_{ti} between the roller and the screw.

The force applied to each thread is obtained [13] as follows:

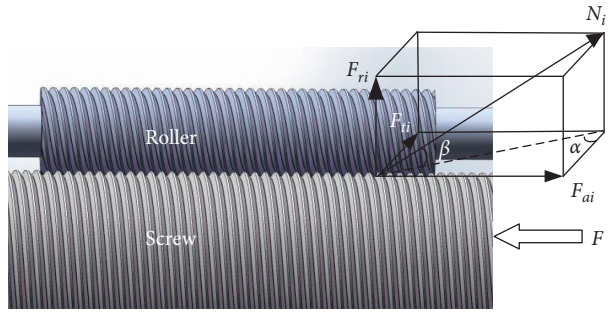

Figure 2: Diagram of screw and roller contact force.

$$\begin{cases} F_{ai} = N_i \cdot \cos\beta \cdot \sin\alpha, \\ N_{i-1}^{2/3} = N_i^{2/3} + \dfrac{Np\left(A_s + A_n\right)}{4E_{rs}A_sA_n\left(C_s + C_n\right)}(\sin\alpha)^2(\cos\beta)^2 \sum_{n=i}^{\tau} N_n, \\ N \cdot \sum_{i=1}^{\tau} F_{ai} = F, \end{cases} \tag{1}$$

where α is the contact angle of the lead screw thread teeth, β is the screw angle of the roller thread, τ refers to the number of roller thread turns, N is the roller number, E_{rs} is the equivalent Young's modulus of the lead screw and roller, C_s is the lead screw rigidity, C_n is the nut rigidity, A_s is the effective contact area of the lead screw, A_n is the effective contact area of the nut, p is the pitch, and F is the load of the roller screw mechanism.

2.2. Friction Torque of PRSM

2.2.1. Friction Torque Caused by Elastic Hysteresis. In the work process of the roller screw mechanism, the roller thread teeth rolls forward with respect to the lead screw thread teeth as a reference body. The roller thread is in contact with the lead screw thread. The actual shape of the contact point is a space ellipse according to Hertz contact theory (Figure 3).

The contact ellipse position is constantly changing due to the relative movement of the roller and lead screw. According to Hertz contact theory, as long as the position of the contact ellipse changes, the roller thread produces elastic hysteresis deformation and energy is lost.

The friction moments of the first mechanism of the lead screw-roller and nut-roller mechanism thread teeth due to elastic lag are derived [13] as follows:

$$\begin{cases} M_{ei} = \dfrac{3}{8}\gamma B m_{bs} a_s N_i, \\ M'_{ei} = \dfrac{3}{8}\gamma B m_{bn} a_n N_i, \end{cases} \tag{2}$$

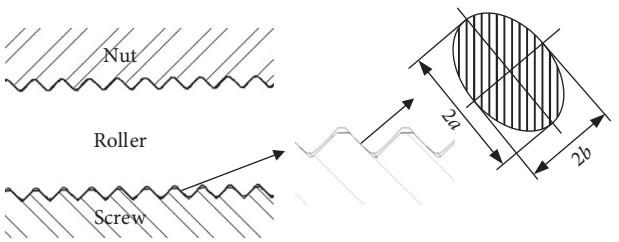

Figure 3: Contact ellipse of PRSM.

where γ is the material energy loss coefficient, B is the dimensionless coefficient, m_{bs} and m_{bn} are the elliptic eccentricity coefficients, a_s is the lead screw-roller mechanism's contact elliptic long half shaft, and a_n is the contact ellipse long half shaft of the nut-roller mechanism.

2.2.2. Friction Torque Caused by Spinning Sliding. In the work process of the roll lead screw, the roller and lead screw always have the relative angular velocity in the normal contact direction. The relative angular velocity causes spinning sliding and brings the friction moment. The respective spinning sliding friction moments M_{si} and M'_{si} of the screw-roller and nut-roller mechanisms consisting of a single mechanism of the lead screw, roller thread, and nut and roller threads can be derived [8] as

$$\begin{cases} M_{si} = \cos\alpha \cdot \iint f_s \dfrac{3N_i}{2\pi a_s b_s}\left(1 - \dfrac{x^2}{a_s^2} - \dfrac{y^2}{b_s^2}\right)\left(x^2 + y^2\right)^{1/2} \mathrm{d}x\,\mathrm{d}y, \\ M'_{si} = \cos\alpha \cdot \iint f_s \dfrac{3N_i}{2\pi a_n b_n}\left(1 - \dfrac{x^2}{a_n^2} - \dfrac{y^2}{b_n^2}\right)\left(x^2 + y^2\right)^{1/2} \mathrm{d}x\,\mathrm{d}y, \end{cases} \tag{3}$$

where f_s is the sliding friction coefficient between parts, b_s is the contact ellipse short half shaft of the lead screw-roller mechanism, and b_n is the contact ellipse short half shaft of the nut-roller mechanism.

2.2.3. Friction Torque Caused by Differential Sliding. Differential sliding, also known as slight sliding, occurs due to the speed difference between the roller and the lead screw, resulting in a corresponding friction torque. The differential sliding friction moments produced by a single mechanism of the lead screw, roller thread, and nut-roller thread are [19] written as follows:

$$\begin{cases} M_{di} = \dfrac{0.08 f_s N_i a_s^2}{16 f^2 R^2}(2f+1)^2 R_s, \\ M'_{di} = \dfrac{0.08 f_s N_i a_s^2}{16 f^2 R^2}(2f+1)^2 \left(R_s + 2R_r\right), \end{cases} \tag{4}$$

where f is the raceway curvature coefficient, R_s is the lead screw radius, and R_r is the roller radius.

2.2.4. Friction Moment Generated by Viscosity of Lubricating Oil. A lubricant can be found in the roller screw set. When a relative movement occurs among the screw, roller, and nut, a viscous resistance exists between the lubricants attached to the respective parts due to the viscosity, which also brings about frictional torque.

Each roller thread is equivalent to a ball of equivalent diameter; the viscous resistance of the roller screw mechanism can be obtained by comparing the calculation formula of the viscous resistance between the ball and the raceway [20]:

$$F_V = 2.86E\left(\sum \rho\right)_S^2 k^{0.348} G^{0.022} U^{0.66} W^{0.47}, \tag{5}$$

where E is the equivalent elastic modulus of the lead screw and roller or the roller and nut and k is the radius ratio of curvature given by

$$k = \frac{f \cdot R}{(2f-1)R_X}. \tag{6}$$

G, U, and W are dimensionless parameters related to the material, speed, and load, respectively; they can, respectively, be calculated as follows:

$$G = E\alpha_p, \tag{7}$$

$$U = \frac{\eta_0 v}{E R_X}, \tag{8}$$

$$W = \frac{N}{E R_X^2}, \tag{9}$$

where α_p is the viscosity pressure coefficient of the lubricant, η_0 is the dynamic viscosity of the lubricant, and v is the tangential speed of the roller in the raceway direction:

$$v = \frac{\pi n}{30}\left[1 - \left[\frac{d_W \cdot \cos\alpha}{d_m}\right]^2\right] \cdot \frac{d_m}{4}. \tag{10}$$

The viscous resistance caused by the lubricant can be obtained by combining equations (5)–(10). Many involved parameters are utilized, and the detailed calculations are shown in [21]. The viscous resistance moment M_{vi} between a single mechanism of a lead screw and roller thread and the viscous resistance moment M'_{vi} between a single mechanism of the nut and roller thread are as follows:

$$\begin{cases} M_{vi} = F_{vi} R_s, \\ M'_{vi} = F_{vi}\left(R_s + d_r\right). \end{cases} \tag{11}$$

In summary, the friction moment of the lead screw-roller mechanism M_s and the friction moment of the nut-roller mechanism M_n are obtained:

$$\begin{aligned} M_s &= M_{es} + M_{ss} + M_{ds} + M_{vs} \\ &= N \cdot \sum_{i=1}^{\tau}\left(M_{ei} + M_{si} + M_{di} + M_{vi}\right), \end{aligned} \tag{12}$$

$$\begin{aligned} M_n &= M_{en} + M_{sn} + M_{dn} + M_{vn} \\ &= N \cdot \sum_{i=1}^{\tau}\left(M'_{ei} + M'_{si} + M'_{di} + M'_{vi}\right), \end{aligned} \tag{13}$$

where M_{ej}, M_{sj}, M_{dj}, and M_{vj} ($j = s$ and n) are the friction moments caused by the elastic hysteresis of the material, spin slip, differential sliding, and viscous resistance of the lubricant in the lead screw-roller mechanism, respectively.

The total friction torque of the PRSM is

$$M = M_s + M_n. \tag{14}$$

2.3. Friction Torque of PRSM in Fault Mode. The relative motion between the roller and the lead screw and nut constitutes a sliding friction mechanism when the roller only revolves around the lead screw due to failure and does not rotate itself. In this state, the friction force between the single faulty roller and the lead screw and nut can be expressed as follows:

$$F_{hs} = F_{hn} = \sum_{i=1}^{\tau} f_s \cdot N_i. \tag{15}$$

The friction moments of a single faulty roller and lead screw and nut are as follows:

$$\begin{cases} M_{hs} = F_{hs} R_s, \\ M_{hn} = F_{hn} (R_s + 2R_r). \end{cases} \tag{16}$$

Assume N rollers in the roller screw mechanism and the failure of x rollers. The friction moment $M_s(x)$ of the screw-roller mechanism and the friction moment $M_n(x)$ of the nut-roller mechanism are, respectively, derived as follows:

$$\begin{cases} M_s(x) = \dfrac{(N-x)M_s}{N} = M_{hs} x, \\ \\ M_n(x) = \dfrac{(N-x)M_n}{N} + M_{hn} x. \end{cases} \tag{17}$$

In the event of roller failure, the friction torque of the planetary roller-lead screw mechanism is derived as follows:

$$M(x) = M_s(x) + M_n(x). \tag{18}$$

3. Results of Calculation and Analysis

In this work, the parameters of the roller screw mechanism with a lead screw diameter of 27 mm are taken as an example (Table 1).

The load distribution curve of each thread can be obtained by substituting the screw mechanism parameters in equation (1) and compiling the solution program with MATLAB (Figure 4). The maximum and minimum loads are 249.5 and 243.4 N, respectively. Therefore, the load fluctuation changes slightly and can be considered to have a uniform distribution.

The last few turns of the roller thread load increase because this part of the thread is subjected to the additional torque on the front thread, resulting in a tight thread contact.

Given the examples of parameters in Table 1 and the combination of equations (1), (14), and (17), the friction torque of a single normal roller and the law of variation with load are plotted in Figure 5(a). In addition, the friction torque of a faulty roller with different proportions is plotted in Figure 5(b).

Figure 5(a) shows that when the motion pattern of the roller and lead screw changes from pure rolling to pure sliding, the friction torque of the single roller and lead screw sharply increases. The latter is approximately 20 times that of the former. In the lead screw-roller mechanism, the change of friction torque in the case of the failure of the revolution of several rollers can be analyzed from Figure 5(b). The friction torque of the lead screw-roller mechanism increases when the number of rollers with the aforementioned failure is high. When three faulty rollers are present, that is, the number of faulty rollers accounts for 30% of the total, the friction torque of the screw-roller mechanism becomes 6.6 times the normal value. The friction moment of the screw-roller mechanism reaches 0.845 N·m when the load is rated dynamic load.

The friction torque of the roller after pure sliding is much larger than that under normal operation. This difference indicates that the transmission efficiency of the planetary roller screw rapidly drops when the roller is jamming.

3.1. Analysis of Transmission Efficiency. Assume that the efficiency loss of a mechanical structure is caused by friction torque. The ratio of output torque to input torque of the planetary roller screw is efficiency, as shown in the following formula:

$$\eta = \frac{M_{\text{out}}}{M_{\text{in}}} = \frac{M_{\text{out}}}{M_{\text{out}} + M_s + M_n} = \frac{F \cdot p/(2\pi)}{(F \cdot p/(2\pi)) + M_s + M_n}, \tag{19}$$

where p is the lead of the roller screw mechanism; M_{out} is the output torque of the roller-lead screw mechanism, which can be calculated by load and lead; and M_{in} is the input torque of the roller-lead screw mechanism and is equal to the output torque plus friction torque.

Based on the calculation in Section 2 and in equation (19), Figure 6 shows the efficiency change of the roller-lead screw mechanism when the number of jamming rollers changes under the 15 kN load.

(1) The model is established and imported. SolidWorks is used to establish the screw, roller, and nut and complete the assembly. Figure 7 shows the model.

(2) After meshing, the contact mechanisms are set up for the model. Twenty contact mechanisms are set in the model. The screw-roller and nut-roller mechanisms are set with contact mechanisms (Figure 8). In the subsequent analysis, the friction coefficient must be set. The sliding friction coefficient is $f_s = 0.2$, and the rolling friction coefficient is $f_r = 0.1$ [22].

(3) The boundary conditions are added.

The figure shows that under load N_i of 15 kN, the efficiency of the roller screw mechanism decreases from 98.2% to 53.2% as the number of jamming rollers increases from 1 to 10.

Table 1: Example parameters of roller screw mechanism (screw diameter of 27 mm).

Parameters	d_n	d_m	p	β	n_s	τ	Energy loss coefficient
Values	9 mm	45 mm	1 mm	3.8°	5	30	0.008
Parameters	α	N	F	f_m	f_k	E_{rs}	μ
Values	45°	10	5800 N	0.75	43 $N^{2/3}$/mm	210 GPa	0.27

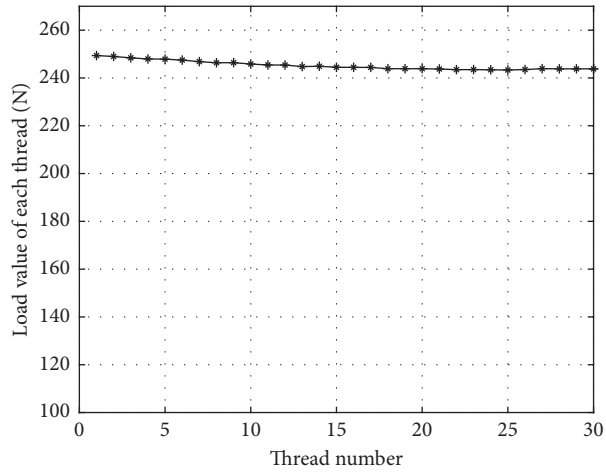

Figure 4: Load value of the roller thread of roller screw mechanism.

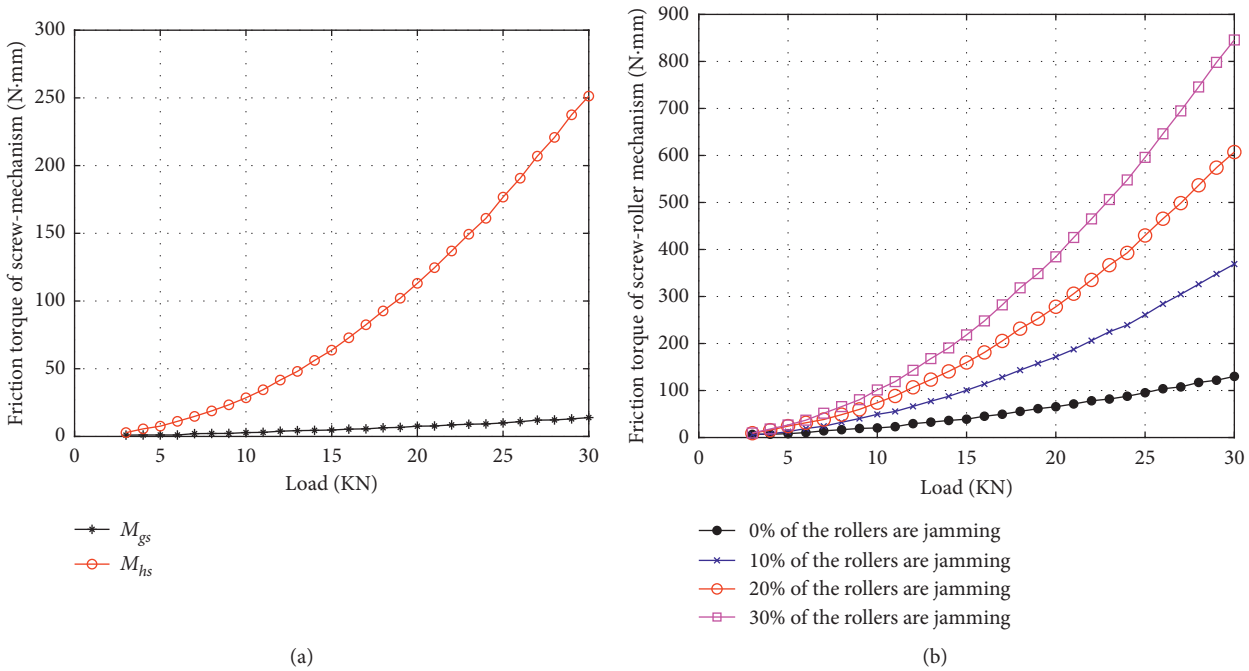

Figure 5: Friction torque in the roller jamming mode.

3.2. Finite Element Analysis of PRSM Contact. A PRSM stress analysis is carried out using the ANSYS Workbench software. The static structural field analysis is mainly used to analyze and calculate the stress field of the PRSM.

Axial loads and constraints are added. The following constraints are added to the PRSM model in the analysis to simulate the movements of the nut with only axial displacement, the roller with rotation and axial displacement, and the screw with only rotation displacement:

(1) The nut only has axial displacement degrees of freedom, and it has no degrees of freedom in other directions.

(2) The roller has axial displacement degrees of freedom.

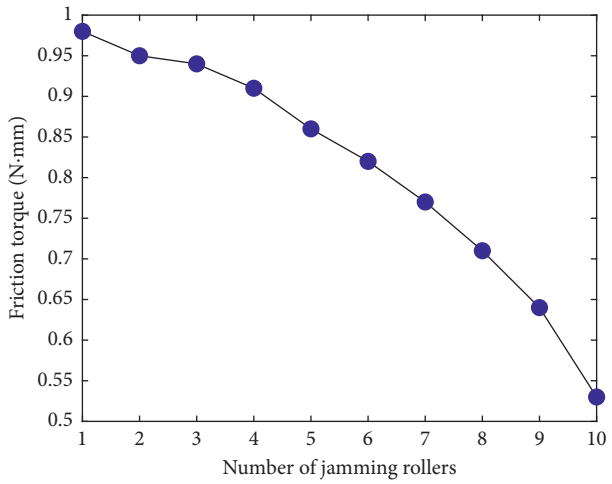

Figure 6: Relationship between efficiency and the number of jamming rollers.

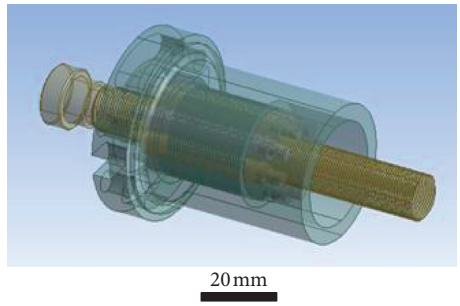

Figure 7: 3D model of PRSM.

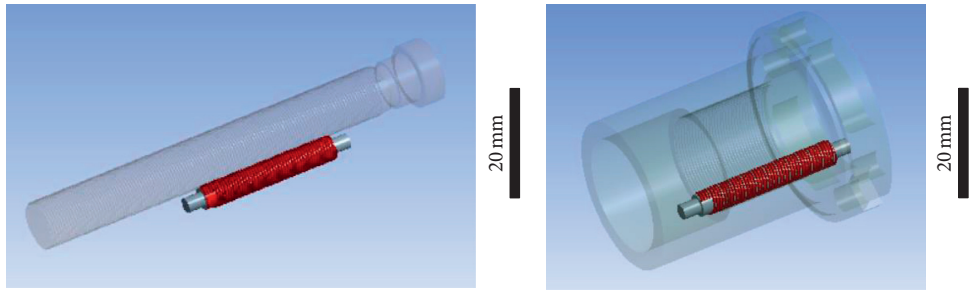

Figure 8: Contact mechanisms of (a) roller-screw mechanism and (b) roller-nut mechanism.

(3) Axial degrees of freedom are present on the end face of the load application side of the lead screw. No displacement degrees of freedom exist in the other three directions.

(4) The roller has rotational freedom around its central axis.

(5) The lead screw has a rotational degree of freedom around its central axis.

Figure 9 shows that the stress concentration appears in the end of the screw and nut and that the stress distribution of the other threads is relatively uniform. The mean von Mises stress of the screw thread is 496.01 MPa and that of the nut thread is 210.11 MPa. The maximum stress value is 892.67 MPa, which is less than the yield stress of 1700 MPa [23].

Take the contact stress of the roller-screw mechanism as an example. The number of jamming rollers is increased to change their friction coefficient. The average stress and friction torque calculated by MATLAB are incorporated in Figure 10. The trend of the mean von Mises stress is positively correlated with friction moment. This result indirectly validates the accuracy of the roller jamming model.

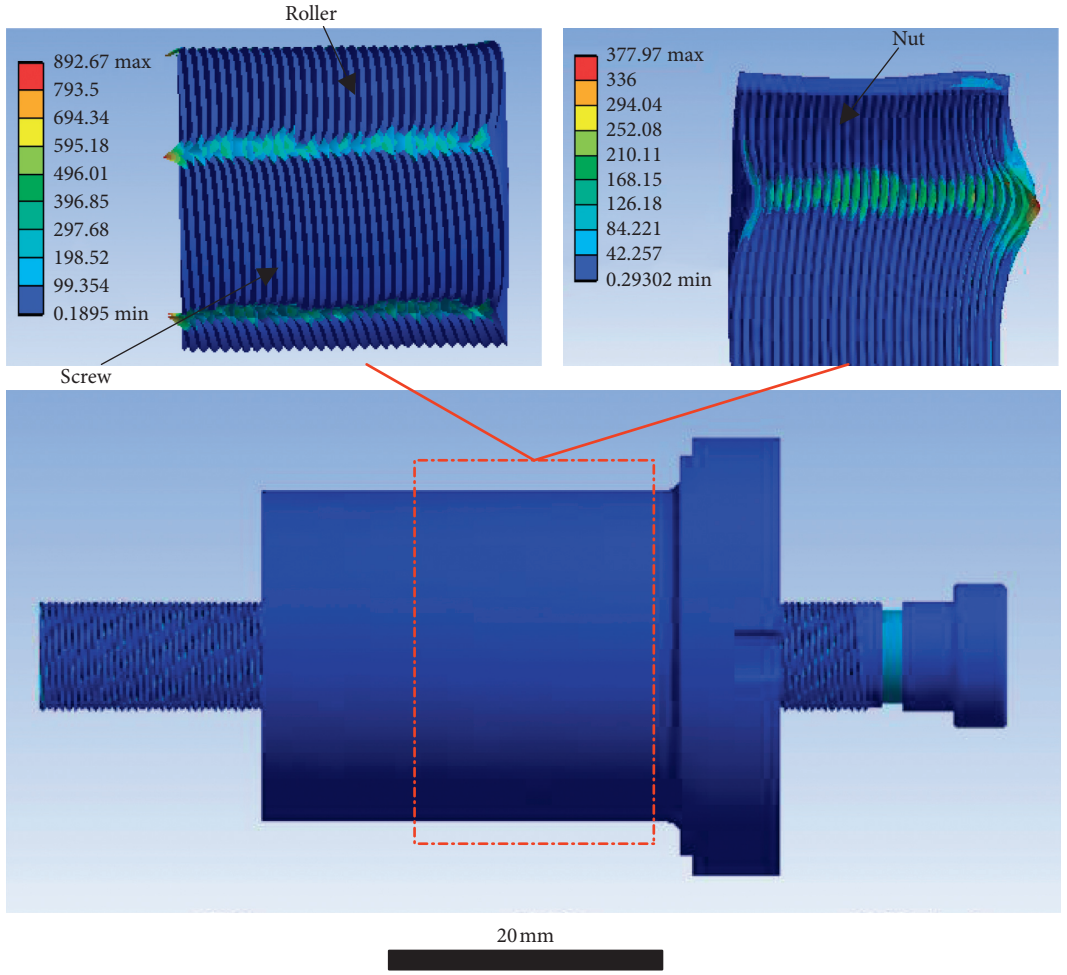

Figure 9: Diagram of von Mises stress distribution of PRSM.

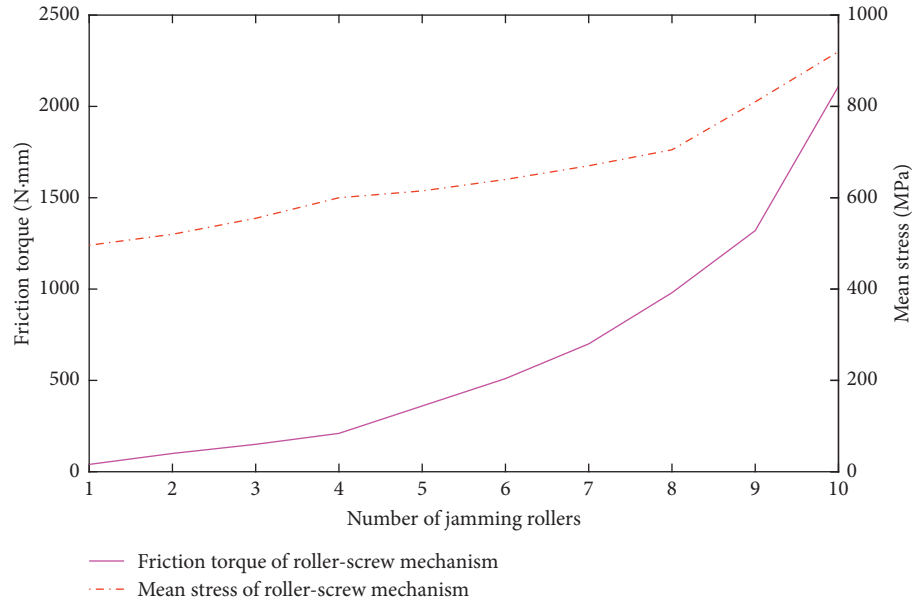

Figure 10: Trend of friction torque and mean stress during roller-screw mechanism jamming.

4. Conclusion

The uneven distribution of the axial load of a planetary roller screw shaft among several rollers exerts an important influence on the smoothness, wear, and life of the PRSM. The uneven load distribution leads to a large transmission noise, increased wear, shortened life, and even jamming.

The following results are obtained by modeling and analyzing the friction torque of the PRSM in roller jamming:

(1) The friction torque of the roller lead screw nonlinearly increases with the change of the external load.

(2) When the roller is jammed and slides with the lead screw and nut, the friction torque of the roller lead screw mechanism greatly increases for each additional jamming roller.

(3) When the roller is jamming, the transmission efficiency decreases from 98.2% to 53.2%.

This proposed roller jamming model can be used to estimate the friction torque of the PRSM system. Experiments will be conducted to study the influences of varying roller jamming conditions and dynamic imbalance on friction torque to validate the roller jamming model.

Data Availability

The data used to support the findings of this study are available from the corresponding author upon request.

Conflicts of Interest

The authors declare that they have no conflicts of interest.

Acknowledgments

This work was supported by the Foundation of China Civil Aircraft Project.

References

[1] A. Garcia, J. Cusido, J. A. Rosero, J. A. Ortega, and L. Romeral, "Reliable electro-mechanical actuators in aircraft," *IEEE Aerospace and Electronic Systems Magazine*, vol. 23, no. 8, pp. 19–25, 2008.

[2] J.-C. Maré and J. Fu, "Review on signal-by-wire and power-by-wire actuation for more electric aircraft," *Chinese Journal of Aeronautics*, vol. 30, no. 3, pp. 857–870, 2017.

[3] S. Guo, J. Chen, Y. Lu, Y. Wang, and H. Dong, "Hydraulic piston pump in civil aircraft: current status, future directions and critical technologies," *Chinese Journal of Aeronautics*, vol. 33, no. 1, pp. 16–30, 2020.

[4] J. Fu, J.-C. Maré, and Y. Fu, "Modelling and simulation of flight control electromechanical actuators with special focus on model architecting, multidisciplinary effects and power flows," *Chinese Journal of Aeronautics*, vol. 30, no. 1, pp. 47–65, 2017.

[5] Y. Wang, S. Guo, and H. Dong, "Modeling and control of a novel electro-hydrostatic actuator with adaptive pump displacement," *Chinese Journal of Aeronautics*, vol. 33, no. 1, pp. 365–371, 2018.

[6] Exlar Roller Screw Technology, http://exlar.com/resources/.

[7] P. E. Dupont, "Friction modeling in dynamic robot simulation," in *Proceedings of the IEEE International Conference on Robotics & Automation*, vol. 1, pp. 1370–1377, Cincinnati, OH, USA, May 1990.

[8] Y. Hojjat and M. Mahdi Agheli, "A comprehensive study on capabilities and limitations of roller-screw with emphasis on slip tendency," *Mechanism and Machine Theory*, vol. 44, no. 10, pp. 1887–1899, 2009.

[9] S. A. Velinsky, B. Chu, and T. A. Lasky, "Kinematics and efficiency analysis of the planetary roller screw mechanism," *Journal of Mechanical Design*, vol. 131, no. 1, pp. 881–889, 2009.

[10] M. H. Jones and S. A. Veinsky, "Contact kinematics in the roller screw mechanism," *Journal of Mechanical Design*, vol. 135, no. 5, pp. 142–151, 2013.

[11] M. H. Jones and S. A. Veinsky, "Dynamics of the planetary roller screw mechanism," *Journal of Mechanisms and Robotics*, vol. 8, no. 1, pp. 1–6, 2016.

[12] W. Zhang, G. Liu, R. Tong, and S. Ma, "Load distribution of planetary roller screw mechanism and its improvement approach," *Proceedings of the Institution of Mechanical Engineers, Part C: Journal of Mechanical Engineering Science*, vol. 230, no. 18, pp. 3304–3318, 2016.

[13] J. Yang, B. Yang, J. S. Zhu, and W. Du, "Effect of preload on axial deformation and friction of planetary roller screw," *Journal of Mechanical Transmission*, vol. 35, no. 12, pp. 16–21, 2011.

[14] Y. Li, J. Yang, W. Liao, and J. Zhu, "Influence of lead angle and contact angle on transmission efficiency of planetary roller screws," *Journal of Hubei University of Technology*, vol. 29, no. 1, pp. 87–91, 2014.

[15] S. Ma, G. Liu, R. Tong, and X. Zhang, "A new study on the parameter relationships of planetary roller screws," *Mathematical Problems in Engineering*, vol. 2012, Article ID 340437, 29 pages, 2012.

[16] S. Ma, G. Liu, and R. Tong, "The frictional moment and transmission efficiency of planetary roller screw," *Journal of Harbin Institute of Technology*, vol. 11, pp. 74–79, 2013.

[17] S. Ma, G. Liu, R. Tong, and X. Fu, "A frictional heat model of planetary roller screw mechanism considering load distribution," *Mechanics Based Design of Structures and Machines*, vol. 43, no. 2, pp. 164–182, 2015.

[18] J. Pu and Y. Fan, "Analysis and experiment of ultimate bearing capacity of ball screw," in *Proceedings of the International Conference on Mechanical Engineering and Mechanics*, vol. 8, Yangzhou, China, August 2014.

[19] C. Wan, *Analysis Method of Rolling Bearing*, Machinery Industry Press, Beijing, China, 1985.

[20] D. Olaru, G. C. Puiu, L. C. Balan, and V. Puiu, "A new model to estimate friction torque in a ball screw system," in *Product Engineering*, pp. 231–240, Springer, Berlin, Germany, 2004.

[21] T. Zhu, *Grease Technology*, China Petrochemical Press, Beijing, China, 2009.

[22] S. Ma, L. Wu, X. Fu, Y. Li, and G. Liu, "Modelling of static contact with friction of threaded surfaces in a planetary roller screw mechanism," *Mechanism and Machine Theory*, vol. 139, pp. 212–236, 2019.

[23] L. Zu, Z. Zhang, and L. Gao, "Design and bearing characteristics of planetary roller screws based on aerospace high-load conditions," *Advances in Mechanical Engineering*, vol. 10, no. 11, pp. 1–11, 2018.